



# Review on Heart-Rate Estimation from Photoplethysmography and Accelerometer Signals During Physical Exercise

Vijitha Periyasamy<sup>1</sup>, Manojit Pramanik<sup>1\*</sup> and Prasanta Kumar Ghosh<sup>2\*</sup>

**Abstract** | Non-invasive monitoring of physiological signals during physical exercise is essential to customize the exercise module. Photoplethysmography (PPG) signal has often been used to non-invasively monitor heart-rate, respiratory rate, and blood-pressure among other physiological signals. Typically, PPG signal is acquired using pulse oximeter from finger-tip or wrist. Advantage of wrist-based PPG sensors is that it is more convenient to wear. Other sensors such as accelerometer can also be integrated with it due to large area on the wrist. This article provides a review of the algorithms developed for heart rate estimation during physical exercise from the PPG signals and accelerometer signals. The datasets used to develop these techniques are described. Algorithms for denoising of PPG signals using accelerometer signals are either in time domain or frequency domain.

**Keywords:** Heart-rate monitoring, Spectral peak tracking, Accelerometer signal, Motion artifact, Physical activity

## 1 Introduction

Real-time heart rate (HR) estimation from the photoplethysmography (PPG) signals is a key step in developing wearable devices that can monitor the HR in a non-invasive way.<sup>1</sup> The PPG signal is obtained from pulse oximeters and its periodicity corresponds to the cardiac rhythm.<sup>2</sup> Oximeters are designed with a light source and detector placed either in reflection mode or in transmission mode (Fig. 1a). Light of wavelength between 500 and 900 nm is illuminated on the skin. The light transmitted or reflected by the skin is proportional to the blood flow (Fig. 1b).<sup>3</sup> Blood flow in the vessels is mediated by the heart beat (Fig. 1c). In spite of the HR information available in the PPG signal, reliable estimation of the HR is not straightforward due to the fact that the PPG signals are vulnerable to motion artifacts (MA), which strongly interfere with the HR. Figure 1d shows a 3-s long PPG signal acquired when the subject is at rest and Fig. 1e shows the same when the subject is exercising on treadmill. Figure 1f, g shows the respective tri-axial accelerometer data.

In comparison, Electrocardiogram (ECG) signals shown in Fig. 1h, i are more robust to MA. MA in PPG during exercise is strong compared to the resting data. Depending on the type of physical activity of the user, the MA component can completely mask the HR information in the PPG signals causing the HR monitoring from the PPG signal challenging.<sup>4,5</sup> Effective MA removal techniques are required for PPG signals acquired during physical exercise to accurately find the HR information. The steps involved in HR estimation using accelerometer information are shown in the block diagram (Fig. 1j).

A typical approach in estimating HR in the presence of MA is to first remove MA from the PPG signal. There are several techniques in the literature for removing MA from the PPG signal.<sup>6</sup> Some of these techniques do not require motion information from an accelerometer while some others do. Independent component analysis (ICA) is one technique where motion data are not required; however, it requires multiple PPG sensors.<sup>7</sup> ICA has been proposed in both time

<sup>1</sup> School of Chemical and Biomedical Engineering, Nanyang Technological University, Singapore 637459, Singapore.

<sup>2</sup> Electrical Engineering, Indian Institute of Science, Bangalore 560012, India.  
\* manojit@ntu.edu.sg;  
prasantg@ee.iisc.ernet.in

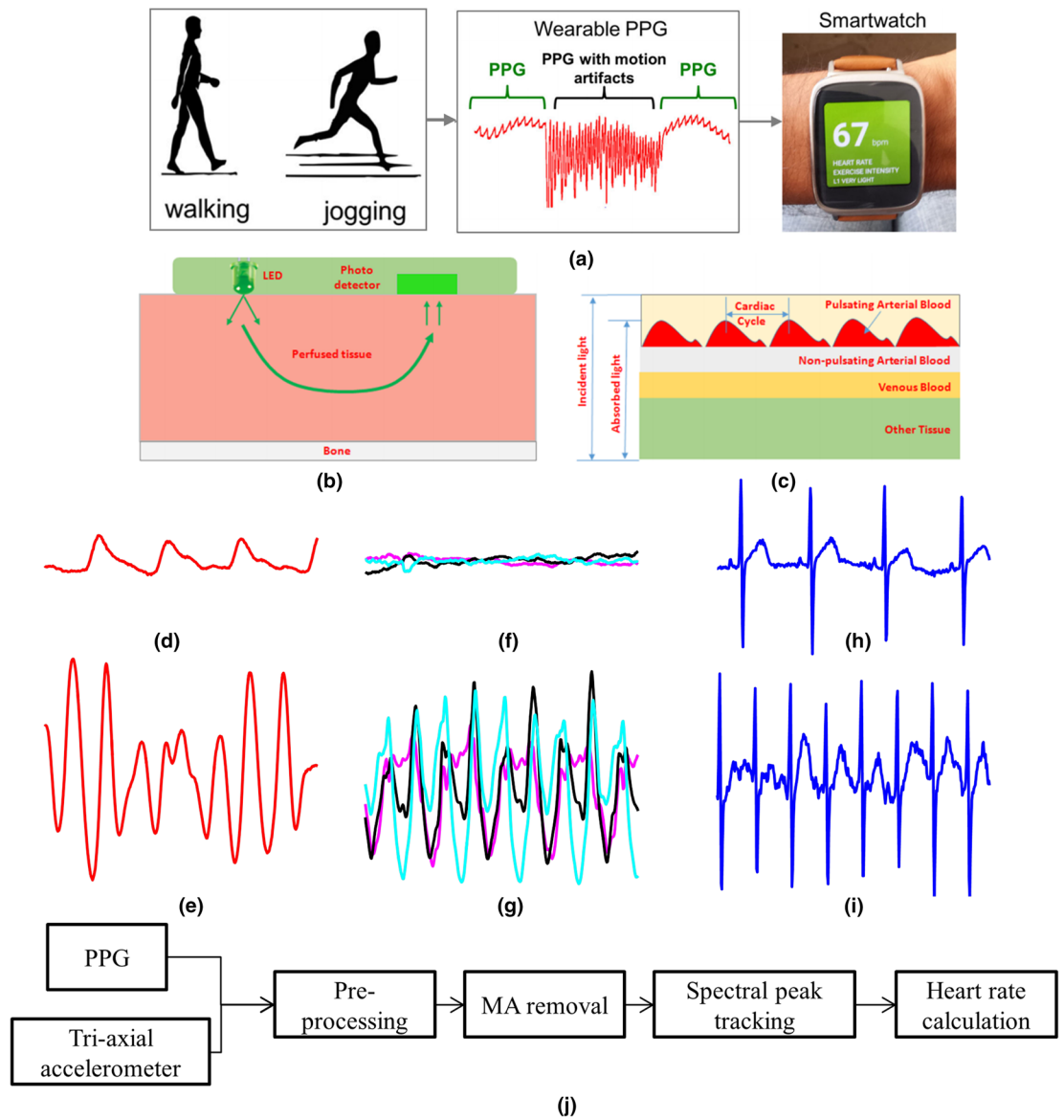


**Figure 1:** **a** Acquisition of PPG signal,<sup>3</sup> **b** illustration source and detector,<sup>3</sup> **c** components of PPG signal<sup>3</sup>, figures were reproduced with permission, **d** sample PPG signal for 3 s, **e** PPG signal with MA, **f** MA from tri-axial accelerometer during rest, **g** MA from tri-axial accelerometer during exercise, **h** ECG signal during rest, **i** ECG signal during motion, **j** block-diagram of steps involved in HR estimation.

domain<sup>8</sup> and frequency-domain.<sup>9</sup> However, the assumption of statistical independence in ICA does not hold well in PPG signal contaminated by MA.<sup>10</sup> On the other hand, when the acceleration data are available, the MA component is adaptively cancelled from the PPG signal using an adaptive filter following least mean square (LMS),<sup>11</sup> normalized LMS,<sup>12,13</sup> fast transversal recursive least square (RLS) algorithms,<sup>14</sup> as well as spectrum subtraction technique,<sup>15</sup> and Laguerre basis function-based signal representation.<sup>16</sup> Other MA removal techniques include electronic processing methodology,<sup>17</sup> time-frequency analysis,<sup>18</sup>

wavelet denoising,<sup>19,20</sup> higher order statistics,<sup>9</sup> empirical mode decomposition,<sup>21,22</sup> and random forest-based method<sup>23</sup> to name a few. However, in case of an intense physical exercise, most of these techniques do not work well.<sup>10</sup> Acceleration data have also been used for the observation model for Kalman filter<sup>24</sup> as well as for Kalman smoother<sup>25</sup> to remove MA. The acceleration data reflect the hand movement in 3-D space while MA in PPG signal also originates from other sources such as changes of the gap between skin and a pulse oximeters surface which cannot be corrected by using acceleration data.<sup>10</sup>

In contrast to the adaptive filtering,<sup>26</sup> Zhilin et al.<sup>10</sup> have proposed a TROIKA (signal decomposition for denoising, sparse signal Reconstruction for high-resolution spectrum estimation, and spectral peak tracking) framework, where a high-resolution spectrum of the PPG signal is calculated using sparse signal reconstruction following signal decomposition using the singular spectrum analysis (SSA). Spectral peak tracking (SPT) is performed on the reconstructed PPG spectra to estimate the HR, which has been shown to be more accurate compared to other HR estimators. However, the SPT solely depends on the initialization of the HR in the first frame. When a wrongly detected spectral peak is used for initialization, the entire estimated HR trajectory could be different from the actual HR trajectory.

Different MA cancellation algorithms such as adaptive noise cancellation (ANC),<sup>27</sup> Kalman filter (KF), Kalman smoother, as well as sparse reconstruction with SSA decomposition remove MA from the PPG signals to varying degrees. This depends on the nature of the MA cancellation algorithm, filter order, and other chosen parameters. The extent of MA cancellation further affects the SPT-based HR estimation performance.

Spectrum of the denoised signal was used to compute the HR.<sup>10</sup> The initialization of the HR in the first few spectra of the PPG signal is done by selecting the frequency corresponding to the highest intensity, since the periodicity of the PPG signals in the first few seconds corresponds to HR. A window around the initialized HR is used to estimate the HR in future spectra. The window location is updated in each prediction. This leads to tracking of the HR in the successive spectra to lie within the given range of beats per minute (BPM).

In this review, pre-processing techniques are discussed. Pre-processing includes simple steps such as demeaning and bandpass filtering. This is done to remove baseline drift and mask the PPG and accelerometer signal within 20–210 BPM.<sup>28</sup> Removal of MA from PPG using accelerometer signal is done in either time domain or frequency domain. Time domain algorithms include filtering techniques, whereas spectral subtraction is done in frequency domain. Different time domain and frequency domain algorithms developed for MA cancellation and advancements in SPT techniques are discussed. Datasets collected with subject on treadmill are detailed in the next section. The frequency and time domain algorithms developed on the dataset are detailed in Sect. 2. Discussions and conclusion is detailed in Sects. 4 and 5, respectively.

## 2 Datasets

The extent of MA component in PPG signal is not measurable. Hence, comparing the efficiency of PPG denoising algorithms remains a challenge. To estimate the efficiency of MA cancellation algorithms, MA is added to the PPG signal which is termed as synthetic dataset.<sup>29</sup> Algorithms developed on synthetic data do not perform well on real-world data. Real-world datasets were acquired while subjects were on treadmill.<sup>10</sup> Algorithms developed for clinical dataset are beyond the scope of this article.<sup>30</sup>

### 2.1 Synthetic

Target PPG signal is mixed with MA in frequency domain.<sup>29</sup> PPG signal is obtained from a subject's finger-tip in resting state. Two MA signals are extracted from PPG sources using temporally constrained independent component analysis and adaptive filtering.<sup>31</sup> MA signals are added to PPG signals in a proportion. To find the efficiency of the synthesized signal, signal-to-noise ratio (SNR) is computed.

### 2.2 Real-World

Well-documented and open-source data were collected and used by Zhang et al.<sup>10</sup> The collected dataset consists of PPG, tri-axial accelerometer, and ECG signals.<sup>10</sup> All three signals were recorded simultaneously. Dataset 1 was collected from ten male subjects under the age of 18–33. Pulse oximeter of wavelength 609 nm was embedded into a wrist band which also incorporated accelerometer. Single-channel ECG was acquired from the chest. All the signals were sampled at 125 Hz. Signals were acquired for 8 min on a treadmill. The first minute subject was at a speed of 2 km/h, next minute the speed was 4 km/h, then at a speed of 10 km/h for a minute after which the speed was increased to 15–17 km/h for 1–1.5 min Fig. 2a. Then the whole cycle was reversed for next 3.5 min. Subjects were requested to perform intentional movements such as wipe sweat and button the shirt in addition to free swinging of the arm.

Dataset 2 consists of two-channel PPG signals, both at wavelength 515 nm which was embedded into wrist band (which also has accelerometer) to collect the data from 12 subjects on treadmill. Each of the PPG data was acquired for 5 min. Subjects were at rest for first 30 s, then speed was 6 km/h for 1 min and 12 km/h for the next minute after which the speed was slowed to 6 km/h and then increased to 12 km/h for 1 min before resting for 30 s. For one of the subjects, the speed

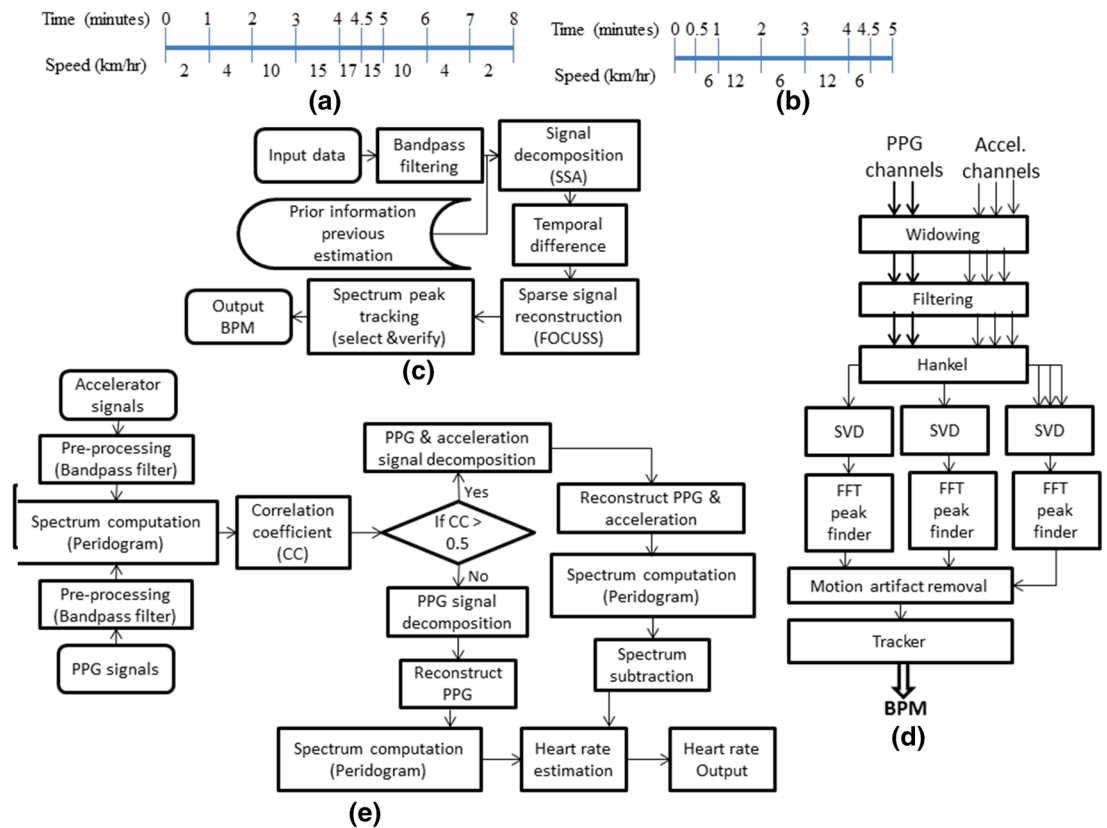


**Figure 2:** **a** Representation of dataset 1, **b** Representation of dataset 2, **c** TROIKA framework,<sup>10</sup> block diagram of **(d)** CARMA<sup>35</sup> and, **e** Empirical mode decomposition.<sup>36</sup>

was 8 and 15 km/h Fig. 2b. ECG signals were also collected during exercise and annotated for heart rate in beats per minute (BPM) over every 8-s time-window which overlapped by 6 s. The advanced dataset was made publicly available as a part of 2015 IEEE signal processing cup (SPC) challenge. This review focusses on the HR estimation algorithms developed for SPC data.<sup>101</sup>

Third set of data were recorded using the set-up by Zhang et al. from eight subjects.<sup>32</sup> Seven subjects were healthy male, while the other female subject had abnormal heart rhythm and blood pressure. Female subject and 3 other subjects performed type 1 exercise which was forearm and upper arm exercise. Six healthy subjects performed type 2 intense exercise such as boxing air. These ten recordings were the test set to validate the algorithms by entrants of the challenge. The HR annotated from ECG is also available. Dataset was developed by Peng et al., with a different set of motions on treadmill. To estimate the efficiency of the MA removal techniques, PPG was acquired from right index finger during four

different motions which are bending of finger at 90°, waving of hand, pressurizing probe clip, and walking each for 20 s.<sup>29</sup> These data were collected from 18 males and 13 females. These activities were performed after 5 min of rest, using two pulse oximeters on each hand at a frequency of 200 Hz. The left hand was stationary on treadmill during the acquisition at a speed of 5 km/h.

### 3 Methods

During the rest state, the periodicity in PPG signal corresponds to the heart beat, but this periodicity is disturbed when the motion artifact interferes. HR estimation, which is a three stage process, begins with bandpass filtering to remove the noise beyond the range of heart beat. The bandpass filtered signal is denoised to remove the motion artifact. Denoising techniques, which are dependent on accelerometer signals, vary from simple filtering to complex sparse reconstruction. Heart rate tracking is the crucial step. HR tracking is done in the frequency domain.

<sup>1</sup> <http://www.zhilinzhang.com/spcup2015>.

### 3.1 Pre-Processing of PPG Signal

Photoplethysmography (PPG) signal is band-pass filtered from 0.5 to 8 Hz.<sup>29</sup> For SPC dataset, PPG signals and accelerometer signals are bandpass filtered from 0.4 to 7 Hz. Usually, HR varies from 40 to 120 BPM, which corresponds to 0.6–3.5 Hz.<sup>10</sup> Butterworth IIR filter was used.<sup>33</sup> This bandpass filtering increases the sparseness in the signals which is an advantage for sparsity-based algorithms and reduces the wandering of HR tracks beyond range. Since PPG was prone to baseline drift due to electronic interference, demeaning and normalizations were also done as a part of pre-processing.<sup>34</sup>

### 3.2 Motion Artifact Removal and HR Estimation

#### 3.2.1 Frequency Domain

TROIKA framework is robust to strong motion artifact.<sup>10</sup> Signal decomposition, sparse signal reconstruction (SSR), and spectral peak tracking (SPT) formed the basis (Fig. 2c). For signal decomposition, the PPG signal is segmented into smaller, overlapping components. Singular spectrum analysis (SSA), single-channel independent component analysis, and empirical mode decomposition are some of the techniques used in the literature; SSA was used in TROIKA. This time domain decomposition involves embedding, singular value decomposition, grouping, and reconstruction. Focal underdetermined system solver algorithm which is used in source localization and direction-of-arrival estimation was used for SSR. SPT involves initialization, peak selection, and trend verification. The verification is dependent on the characteristics of the recorded data and the nature of heart rate. TROIKA is also performed on signals down-sampled at 25 HZ.

TROIKA framework which was considered gold standard was modified for better accuracy.<sup>33</sup> SSA was followed by real-time clustering (RTC), frequency points selection, and prediction followed by multiple-way selection. In the spectrum of denoised signal obtained after SSA, three peaks which were two-thirds the intensity of the maximum were retained. The selected peaks were clustered. Due to the smoothness in the HR, when the cluster of peaks is not close to the previous peak, the previous peak is considered for BPM calculation. BPM for the current frame (beyond first three frames) were dependent on the BPM of two previous HRs. In multiple-way selection, the previous computed HRs were corrected. TROIKA was the first algorithm to use singular spectrum

analysis for MA removal in PPG signals which was improvized further for better accuracy.

CARMA (closest subspace algorithm for reducing motion artifact) depends on singular value decomposition (SVD) of the Hankel matrix obtained after preprocessing the PPG and accelerometer signals (Fig. 2d).<sup>35</sup> Key assumption of this technique was that the artifact and heart rate lie in different subspaces. Adaptive peak tracking was used for HR estimation. Spectrum subtraction is combined with ensemble empirical mode decomposition (EEMD). EEMD decomposes the PPG signal and acceleration signals into intrinsic mode functions (Fig. 2e).<sup>36</sup> Spectrum subtraction is used to remove the spectrum of acceleration signal from PPG signal. In order to increase the resolution of the spectrum for better HR estimation, zero-padding Discrete Fourier Transformation (DFT) followed by KF for tracking of HR.<sup>37</sup> This technique does not require pre-processing, and hence, it is computationally simple. SPECTRAP algorithm has spectrum subtraction, peak tracking, and post-processing. The down-sampled signals were filtered and subjected to symmetric least square-based spectral subtraction. MA spectrum is subtracted from PPG spectrum.<sup>38</sup> Cumulative spectrum (CUMSPEC) technique sparsifies the signal using iterative method adaptive thresholding, followed by median filtering of HR estimates. Genetic algorithm was used for HR tracking.<sup>39</sup> These algorithms were compared with TROIKA.

Gridless spectral estimation and SVM-based peak selection (GRESS) is another algorithm for Zhang's advanced dataset.<sup>40</sup> The conventional estimation of HR in a spectrum which is pixelated is modified. Grid-less spectral estimation is dependent on sparsity of the signal. Peak-to-peak separation distance and amplitude peaks were used to train a two-class support vector machine (Fig. 3a). Gridless spectral estimation helped to overcome the basis mismatch. Basis mismatch was observed in other algorithms which assumed sparsity aligned to specific frequency grids. Spectral peak selection was formulated into a pattern classification task, and hence user-defined parameters were reduced. This algorithm performed better than TROIKA framework for few subjects, but was not as efficient as joint sparse spectrum reconstruction (JOSS). JOSS was once again proposed by Zhilin Zhang. Multiple measurement vector model was used for joint spectral analysis which was followed by spectral subtraction.<sup>41</sup> The peak verification process was intensified as compared to TROIKA.<sup>42</sup> After the peak verification steps of TROIKA, the peak discovery



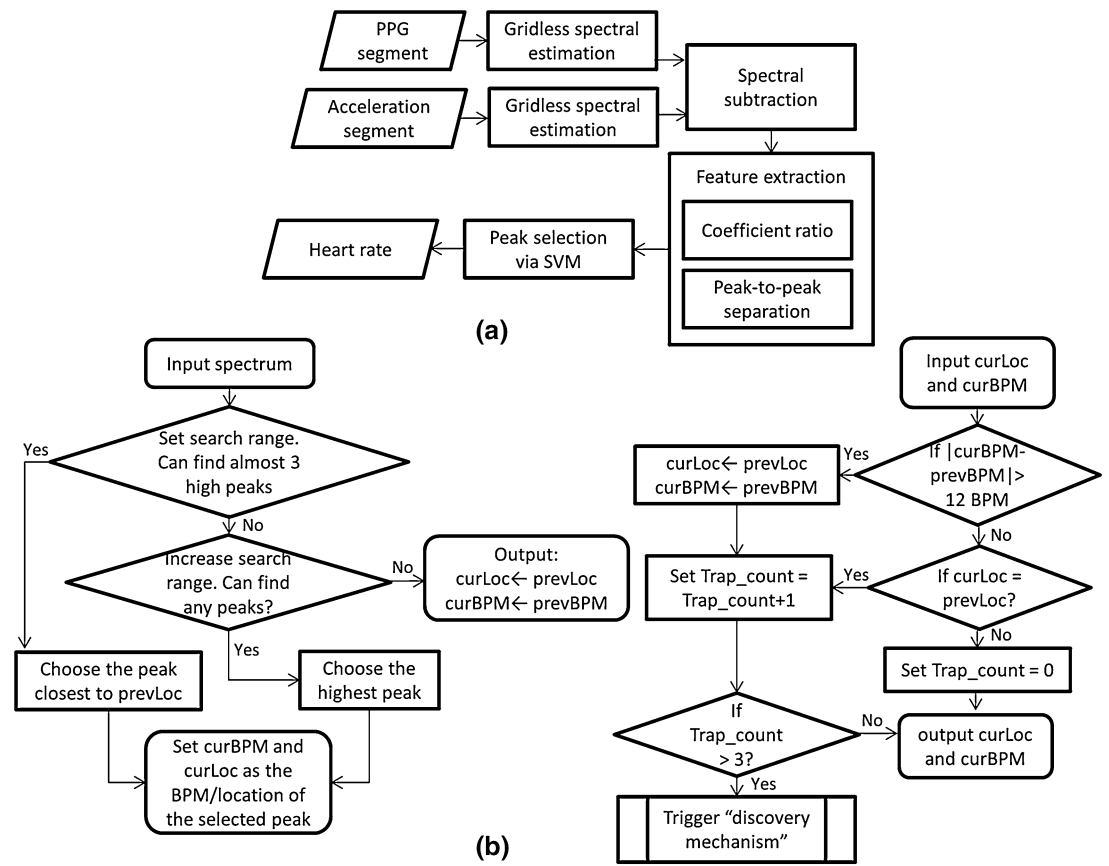


Figure 3: a Block diagram of GRESS<sup>40</sup> and b flow-chart of JOSS.<sup>41</sup>

is incorporated which smooths the selected peak (Fig. 3b). Instantaneous fundamental frequency of acceleration signal is computed using finite harmonic sum (HSUM) (Fig. 4a).<sup>3</sup> The computed fundamental frequency is fitted to the PPG signal, where one of the harmonic sums corresponds to the HR while the harmonics are of MA. In Multi-channel spectral matrix decomposition (MC-SMD) technique, the spectra of PPG signal are divided by the spectrum of acceleration signal (Fig. 4b).<sup>43</sup> This algorithm is compared with 25 Hz JOSS and TROIKA results. MC-SMD is computationally cheap because it does not have a noise-removal module. Short-time Fourier transform (SFST) and spectral analysis is also combined.<sup>44</sup> SFST was robust to frequency variation compared to wavelet transform techniques. Adding a average filter increased the HR estimation.

### 3.2.2 Time Domain

Spectral peak search-comb filtering (SPS-CF) was developed which is dependent on the weighted sum of the delayed signal and bandpass time domain signal.<sup>29</sup> The feed-forward comb filter was evenly spaced peaks in the magnitude

frequency response. Adaptive filters were estimated for removal of MA from PPG signals.<sup>45</sup> The authors used normalized least mean square (NLMS) filter to denoise each of the two PPG signals in advanced Zhang dataset. This leads to six denoised PPG signals. STFT of these signals were multiplied for a single spectrum. HR was estimated from the STFT spectrum by picking the highest intensity representing 40–170 BPM. To maintain the trend, the threshold was set for the chosen BPM. The efficiency of the adaptive filter technique is compared with TROIKA.

Multiple initialization spectral peak tracking (MISPT) has an denoising technique based on adaptive noise cancellation filter and emphasis is laid on peak selection (Fig. 5a).<sup>46</sup> FFT of denoised time domain signal was taken for HR estimation. Initialization was done in each spectral window and the trajectory was generated by back tracking. The trajectory was based on selection of location of maximum intensity within a given window. The HR which corresponded to trajectory of maximum strength was the recorded BPM. This algorithm outperformed TROIKA and JOSS in both 25 and 125 Hz PPG signals.

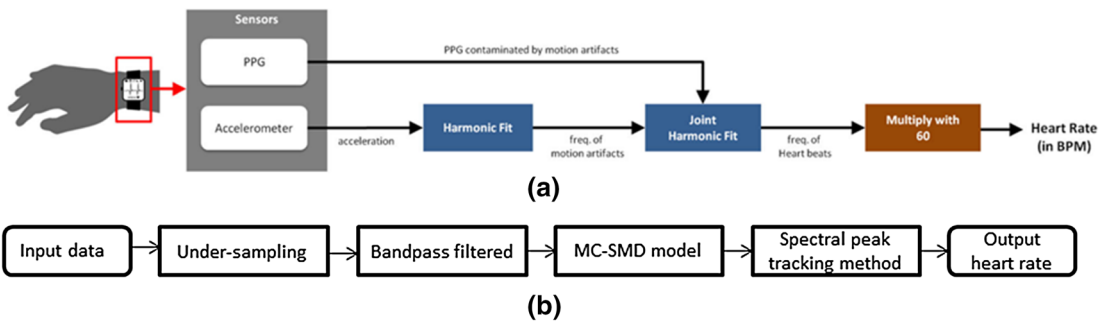


Figure 4: Block diagram of a HSUM<sup>43</sup> and b MC+SMD.<sup>43</sup>

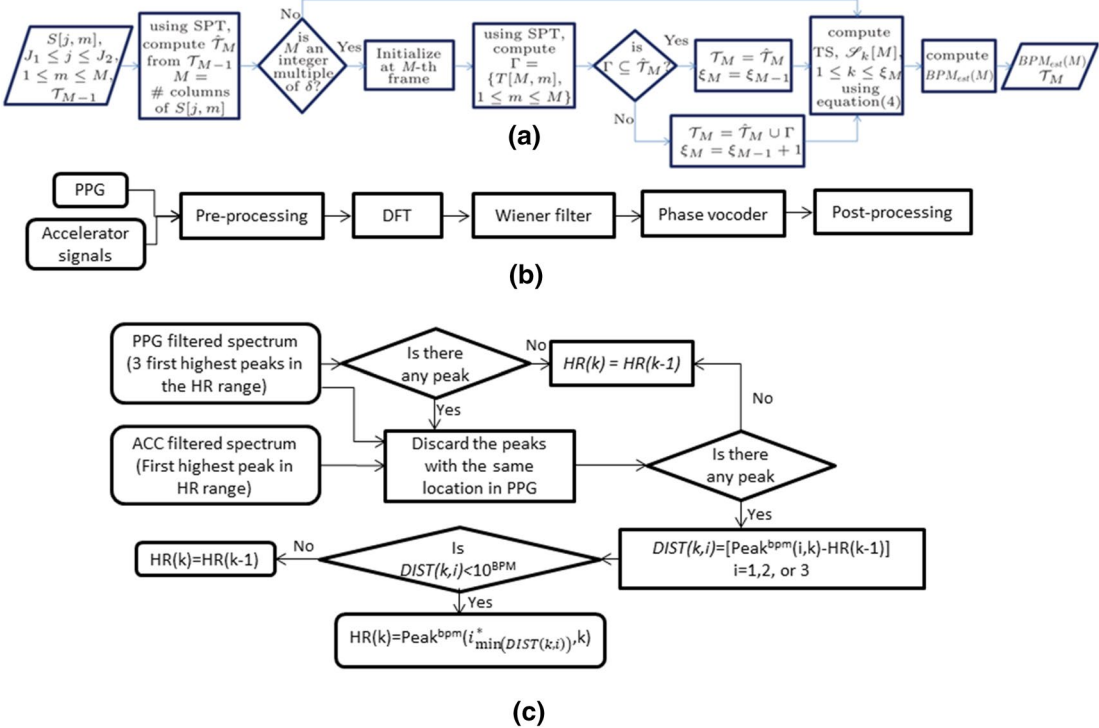
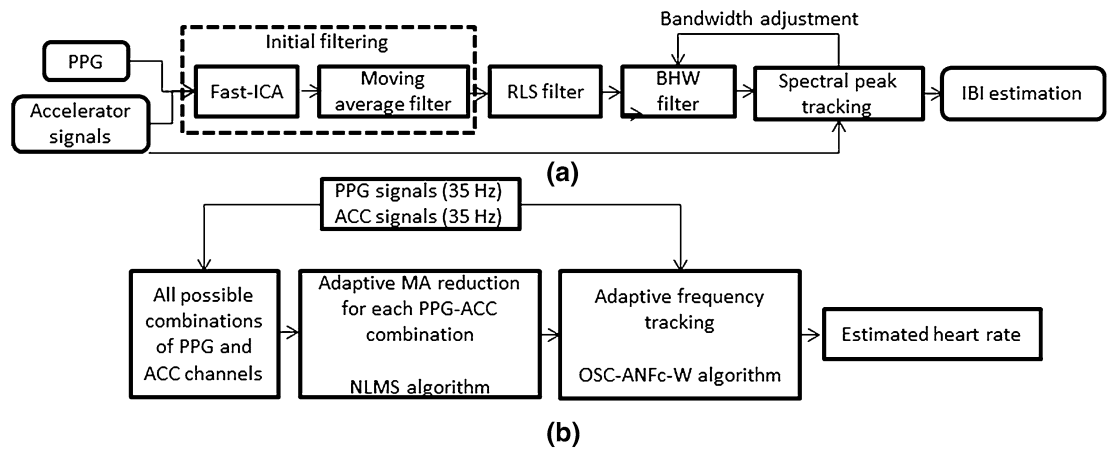


Figure 5: a Flow-chart of MISPT,<sup>40</sup> figure is reproduced with permission, b block diagram of WF+PV,<sup>40</sup> c flow-chart of SpaMA.<sup>49</sup>

One of the three accelerometer signals are chosen based on their highest bandpower. The chosen accelerometer signal is used to filter the PPG signal using RLS filter.<sup>47</sup> Bandpass filtered signals were normalized and averaged (Fig. 5b).<sup>48</sup> These averaged PPG signals and accelerometer signals are down-sampled to 25 Hz. After which DFT is performed and Wiener filtering (WF) is applied to remove MA. To increase the HR estimation accuracy, phases of the chosen peak and the previous peaks are refined. Time-varying spectral comparison of PPG acceleration signal enables the removal of peaks due to MA (SpaMA)

(Fig. 5c).<sup>49</sup> RLS filter and Blackman-Harris-Win-dow was used as pre-processing steps to estimate HR in HEAL-T (Fig. 6a).<sup>50</sup> MURAD- Multiple Reference ADaptive noise cancellation for HR estimation is the algorithm where the denoising of PPG using RLS filter is done individually by the three accelerometer signals and once again by the signal obtained by difference between the two PPG signals.<sup>51</sup> RLS and spectral decomposition (SD) technique was combined for better performance.<sup>32</sup> The key of this algorithm was the use of Bayesian decision for HR estimation. This algo-rithm is compared with 25 Hz TROIKA results.



**Figure 6:** Block diagram of **a** HEAL-T<sup>50</sup> and **b** NLMS+AFT.<sup>50</sup>

Result of NLMS algorithm was further band-pass filtered with discrete oscillator-based adaptive notch filter (OSC-ANF) for instant tracking of changing frequency (Fig. 6b).<sup>52</sup> HR estimation was done using recursive filtering after EEMD.<sup>53</sup> SVD is used for MA cancellation (MAC) and HR was estimated from denoised signal using spectral analysis.<sup>54</sup> Since MA is minimal for the first few seconds, HR estimation in the spectral domain is simple.<sup>41</sup> The frequency corresponding to the maximum spectral intensity converted to beats per minute (BPM) is the heart rate. A window is taken around the initial heart rate while estimation of the HR in the subsequent windows. This is based on the fact that rate of change of HR is gradual. The window location is adaptive over each spectral window to enable gradual rise or fall in the HR. The frequency of optimized spectral peak within the given denoised spectral window is the HR.<sup>29</sup> Estimated HR is also compensated for the directional trend of BPM.

#### 4 Discussion

The results of the existing algorithms are tabulated in Table 1. Performance of both the domains across 12 subjects (dataset 2) is listed. Twelve frequency domains and twelve time domain algorithms are shown. Least error by frequency domain denoising techniques is 0.73 BPM and time domain is 0.97 BPM. Consistently, the error in HR estimation by all the algorithms for subject ten is high. The only exception is HSUM technique.<sup>3</sup> HSUM outperforms all the other algorithms, because it depends on the harmonics of the PPG signals. The harmonics are suppressed by all the other algorithms by bandpass filtering.

This review article is confined to the dataset collected by Zhang et al., because it is specific to the HR estimation when on treadmill. The other algorithms which are developed on datasets which are not available publicly are not discussed in this review.<sup>56–59</sup> The algorithms for which the performance across 12 subjects are not discussed is also excluded from the review since it confines the comparison across algorithms.<sup>60,61</sup> PPG signals were also used to estimate other physiological parameters such as blood pressure and oxygen saturation.<sup>62,63</sup> The details of the algorithms for computation of other physiological parameters are beyond the scope of this review. Heart-rate estimation from PPG acquired using other devices such as mobile phones and laptop cameras from other regions of interest for example forehead, ear is interesting and has its own unique challenge. However, it is beyond the scope of this review here.<sup>64,65</sup>

Estimation of HR from PPG is validated using HR estimated from ECG which is the electrical activity of heart. Since an error of 1 BPM is accepted clinically, three of the discussed algorithms have the potential to replace ECG for heart-rate estimation. PPG is widely used in clinic, and hence, it is safe to use. With advancement of wearable devices, acquisition of PPG signals is getting simpler than acquisition of ECG which has to be collected from a minimum of three electrodes.<sup>66</sup> Another important point to be noted is, with good denoising of PPG signals, that other physiological parameters such as blood oxygen saturation, respiratory rate, and anaesthesia monitoring can also be measured unlike those from ECG.



**Table 1:** Comparison of the error in BPM across various algorithms detailed.

	Sub1	Sub2	Sub3	Sub4	Sub5	Sub6	Sub7	Sub8	Sub9	Sub10	Sub11	Sub12	Avg
Frequency domain													
TROIKA(125) <sup>10</sup>	2.29	2.19	2.00	2.15	2.01	2.76	1.67	1.93	1.86	4.70	1.72	2.84	2.34
TROIKA(25) <sup>10</sup>	2.87	2.75	1.91	2.25	1.69	3.16	1.72	1.83	1.58	4.00	1.96	3.33	2.42
RTC <sup>33</sup>	1.70	2.36	1.00	2.14	0.87	1.96	1.01	0.73	0.86	8.93	1.15	1.88	2.05
CARMA <sup>35</sup>	2.58	1.48	1.40	2.47	1.54	3.24	1.01	1.19	0.93	6.28	1.68	3.30	2.26
EEMD <sup>36</sup>	2.06	3.59	0.92	1.54	0.97	1.64	2.25	0.63	0.62	4.62	1.30	1.80	1.83
DFT + KF <sup>37</sup>	2.11	1.89	1.01	1.08	0.61	1.66	0.54	0.59	0.54	4.12	1.15	2.83	1.51
SPECTRAP <sup>38</sup>	1.18	2.42	0.86	1.38	0.92	1.37	1.53	0.64	0.60	3.65	0.92	1.25	1.39
CUMSPEC <sup>39</sup>	1.81	1.44	0.63	1.16	0.83	1.40	1.02	0.63	0.68	2.77	1.03	0.90	1.19
GRESS <sup>40</sup>	1.18	2.42	0.86	1.38	0.76	1.37	0.72	0.64	0.60	3.65	0.82	1.04	1.45
JOSS <sup>41</sup>	1.33	1.75	1.47	1.48	0.69	1.32	0.71	0.56	0.49	3.81	0.78	1.04	1.28
HSUM <sup>3</sup>	0.61	0.76	0.65	0.59	0.53	0.52	0.59	0.51	0.41	0.58	1.48	1.58	0.73
MC + SMD <sup>43</sup>	1.16	1.07	0.80	1.13	0.98	1.29	0.88	0.81	0.55	3.18	0.79	0.72	1.11
SFST + SA <sup>44</sup>	1.23	1.51	1.19	0.92	0.61	0.78	0.48	0.49	0.58	3.00	0.73	1.24	1.06
Time domain													
NLMS <sup>45</sup>	2.40	1.21	1.20	1.22	1.34	1.44	1.16	1.04	1.18	5.33	2.18	1.52	1.77
MISPT (125) <sup>46</sup>	1.58	1.80	0.58	0.99	0.74	0.93	0.73	0.45	0.41	3.60	0.88	0.68	1.11
MISPT (25) <sup>46</sup>	1.53	2.08	1.30	1.01	0.74	0.97	0.72	0.46	0.42	4.28	0.88	0.69	1.26
RLS <sup>47</sup>	1.34	1.28	0.82	1.37	0.90	1.31	0.95	0.96	0.73	3.01	1.28	0.85	1.23
WF + DFT <sup>48</sup>	1.23	1.26	0.72	0.98	0.75	0.91	0.67	0.91	0.54	2.61	0.94	0.98	1.04
SpaMA <sup>49</sup>	1.23	1.59	0.57	0.44	0.47	0.61	0.54	0.40	0.40	2.63	0.64	1.20	0.89
HEAL-T <sup>50</sup>	3.96	1.73	0.91	2.21	0.32	1.19	0.32	0.47	0.26	4.22	0.87	1.41	1.49
MURAD <sup>51</sup>	1.17	0.93	0.7	0.82	0.88	0.97	0.67	0.74	0.49	2.69	0.81	0.77	0.97
RLS + SD <sup>32</sup>	1.66	1.56	0.65	1.48	0.77	1.12	0.72	0.91	0.42	2.35	1.45	0.78	1.16
OSC-ANF <sup>52</sup>	1.95	1.89	1.64	2.10	1.25	1.62	1.23	1.72	1.27	2.98	1.49	1.37	1.71
EEMD + RLS <sup>53</sup>	1.70	0.84	0.56	1.15	0.77	1.06	0.63	0.53	0.52	2.56	1.05	0.91	1.02
MAC <sup>54</sup>	1.72	1.33	0.90	1.28	0.93	1.41	0.61	0.88	0.59	3.78	0.85	0.71	1.25
NLMS + AFT <sup>55</sup>	1.75	1.94	1.17	1.67	0.95	1.22	0.91	1.17	0.87	2.95	1.15	1.00	1.40

## 5 Conclusion

Electrocardiogram (ECG) is the gold standard for HR estimation. The algorithms discussed here are evaluated with HR estimated from ECG. Hence, the evaluation method of these techniques is proven. The drawback of the current techniques is that it is not validated across different PPG datasets. Since these algorithms developed are independent of the previous estimates, increase of the data acquisition in time may not affect the accuracy. However, the discussed algorithms are not robust to subjects during other tasks or patients data. The performance is expected to vary considerably. The monitoring of the HR is more essential in subjects with cardiac disorders. The robustness of the proposed algorithms across patient database is yet to be validated. Even though the numerous algorithms developed are

real-time, porting these to the embedded device still remains a challenge.

## Acknowledgements

This work was financially supported from the Tier 2 research grant funded by Ministry of Education in Singapore (ARC2/15: M4020238).

Received: 15 February 2017 Accepted: 5 August 2017  
Published online: 22 September 2017

## References

1. Selvaraj N, Jaryal A et al (2008) Assessment of heart rate variability derived from finger-tip photoplethysmography as compared to electrocardiography. *J Med Eng Technol* 32(6):479–484

2. Mendelson Y, Ochs BD (1988) Noninvasive pulse oximetry utilizing skin reflectance photoplethysmography. *IEEE Trans Biomed Eng* 35(10):798–805
3. Dubey H, Kumaresan R, Mankodiya K (2016) Harmonic sum-based method for heart rate estimation using PPG signals affected with motion artifacts. *J Ambient Intell Hum Comput* 1–14
4. Tamura T, Maeda Y et al (2014) Wearable photoplethysmographic sensors past and present. *Electronics* 3(2):282–302
5. Lee J, Jung W et al (2004) Design of filter to reject motion artifact of pulse oximetry. *Comput Stand Interf* 26(3):241–249
6. Han H, Kim M-J, Kim J (2007) Development of real-time motion artifact reduction algorithm for a wearable photoplethysmography. In: 29th annual international conference of the IEEE, Engineering in medicine and biology society, 2007, EMBS 2007. IEEE, New Jersey, pp 1538–1541
7. Yao J, Warren S (2005) A short study to assess the potential of independent component analysis for motion artifact separation in wearable pulse oximeter signals. In: 27th Annual international conference of the engineering in medicine and biology society, 2005, IEEE-EMBS 2005. IEEE, New Jersey, pp 3585–3588
8. Kim BS, Yoo SK (2006) Motion artifact reduction in photoplethysmography using independent component analysis. *IEEE Trans Biomed Eng* 53(3):566–568
9. Krishnan R, Natarajan B, Warren S (2010) Two-stage approach for detection and reduction of motion artifacts in photoplethysmographic data. *IEEE Trans Biomed Eng* 57(8):1867–1876
10. Zhang Z, Pi Z, Liu B (2015) TROIKA: a general framework for heart rate monitoring using wrist-type photoplethysmographic signals during intensive physical exercise. *IEEE Trans Biomed Eng* 62(2):522–531
11. Punalchard R, Benjangkaprasert C et al. (2001) A robust variable step-size LMS-like algorithm for a second-order adaptive IIR notch filter for frequency detection. In: IEEE third workshop on signal processing advances in wireless communications, 2001, (SPAWC'01). IEEE, New Jersey, pp 232–234
12. Chan K, Zhang Y (2002) Adaptive reduction of motion artifact from photoplethysmographic recordings using a variable step-size LMS filter. In: Proceedings of IEEE in sensors, 2002, vol 2. IEEE, New Jersey, pp 1343–1346
13. Han H, Kim J (2012) Artifacts in wearable photoplethysmographs during daily life motions and their reduction with least mean square based active noise cancellation method. *Comput Biol Med* 42(4):387–393
14. Wei P, Guo R et al (2008) A new wristband wearable sensor using adaptive reduction filter to reduce motion artifact. In: International conference on information technology and applications in biomedicine, 2008, ITAB 2008. IEEE, New Jersey, pp 278–281
15. Fukushima H, Kawanaka H et al (2012) Estimating heart rate using wrist-type photoplethysmography and acceleration sensor while running. In: Annual international conference of the IEEE engineering in medicine and biology society (EMBC), 2012. IEEE, New Jersey, pp 2901–2904
16. Wood LB, Asada HH (2006) Active motion artifact reduction for wearable sensors using Laguerre expansion and signal separation. In: 27th Annual international conference of the engineering in medicine and biology society, 2005, IEEE-EMBS 2005. IEEE, New Jersey, pp 3571–3574
17. Hayes MJ, Smith PR (2001) A new method for pulse oximetry possessing inherent insensitivity to artifact. *IEEE Trans Biomed Eng* 48(4):452–461
18. Yan Y-S, Poon CC, Zhang Y-T (2005) Reduction of motion artifact in pulse oximetry by smoothed pseudo Wigner-Ville distribution. *J NeuroEng Rehabil* 2:3
19. Raghuram M, Madhav KV et al (2010) Evaluation of wavelets for reduction of motion artifacts in photoplethysmographic signals. In: 10th International conference on information sciences signal processing and their applications (ISSPA), 2010. IEEE, New Jersey, pp 460–463
20. Foo JYA (2006) Comparison of wavelet transformation and adaptive filtering in restoring artefact-induced time-related measurement. *Biomed Signal Process Control* 1(1):93–98
21. Sun X, Yang P et al (2012) Robust heart beat detection from photoplethysmography interlaced with motion artifacts based on empirical mode decomposition. In: IEEE-EMBS international conference on biomedical and health informatics (BHI), 2012. IEEE, New Jersey, pp 775–778
22. Pinheiro E, Postolache O, Girão P (2012) Empirical mode decomposition and principal component analysis implementation in processing non-invasive cardiovascular signals. *Measurement* 45(2):175–181
23. Ye Y, He W et al (2017) A robust random forest-based approach for heart rate monitoring using photoplethysmography signal contaminated by intense motion artifacts. *Sensors* 17(2):385
24. Lee B, Han J et al (2010) Improved elimination of motion artifacts from a photoplethysmographic signal using a Kalman smoother with simultaneous accelerometry. *Physiol Meas* 31(12):1585
25. Tarvainen MP, Geogiadis SD et al (2006) Time-varying analysis of heart rate variability signals with a Kalman smoother algorithm. *Physiol Meas* 27(3):225
26. Nakajima K, Tamura T, Miike H (1996) Monitoring of heart and respiratory rates by photoplethysmography using a digital filtering technique. *Med Eng Phys* 18(5):365–372
27. Asada HH, Jiang H-H, Gibbs P (2004) Active noise cancellation using MEMS accelerometers for motion-tolerant wearable bio-sensors. In: 26th Annual international conference of the IEEE engineering in medicine and biology society, 2004, IEMBS'04, vol 1. IEEE, New Jersey, pp 2157–2160

28. Islam MT, Ahmed ST et al (2017) Cascade and parallel combination (CPC) of adaptive filters for estimating heart rate during intensive physical exercise from photoplethysmographic signal. *Healthc Technol Lett*
29. Peng F, Liu H, Wang W (2015) A comb filter based signal processing method to effectively reduce motion artifacts from photoplethysmographic signals. *Physiol Meas* 36(10):2159
30. Wadehn F, Carnal D, Loeliger HA (2015) Estimation of heart rate and heart rate variability from pulse oximeter recordings using localized model fitting. In: 37th Annual international conference of the IEEE engineering in medicine and biology society (EMBC), 2015. IEEE, New Jersey, pp 3815–3818
31. Peng F, Zhang Z et al (2014) Motion artifact removal from photoplethysmographic signals by combining temporally constrained independent component analysis and adaptive filter. *Biomed Eng Online* 13(1):1
32. Ye Y, Cheng Y et al (2016) Combining nonlinear adaptive filtering and signal decomposition for motion artifact removal in wearable photoplethysmography. *IEEE Sens J* 16(19):7133–7141
33. Zhang Z-H, Liu J et al (2015) A new framework to extract heart rate information from photoplethysmographic (PPG) signals with strong motion artifacts. In: IEEE region 10 conference TENCN 2015–2015. IEEE, New Jersey, pp 1–4
34. Grisan E, Cantisani G, et al (2015) A supervised learning approach for the robust detection of heart beat in plethysmographic data. In: 37th Annual international conference of the IEEE engineering in medicine and biology society (EMBC), 2015. IEEE, New Jersey, pp 5825–5828
35. Baca A, Biagetti G et al (2015) CARMA: a robust motion artifact reduction algorithm for heart rate monitoring from PPG signals. In: 23rd European signal processing conference (EUSIPCO), 2015. IEEE, New Jersey, pp 2646–2650
36. Zhang Y, Liu B, Zhang Z (2015) Combining ensemble empirical mode decomposition with spectrum subtraction technique for heart rate monitoring using wrist-type photoplethysmography. *Biomed Signal Process Control* 21:119–125
37. Frigo G, Fabris M et al (2015) Efficient tracking of heart rate under physical exercise from photoplethysmographic signals. in: IEEE 1st international forum on research and technologies for society and industry leveraging a better tomorrow (RTSI), 2015. IEEE, New Jersey, pp. 306–311
38. Sun B, Zhang Z (2015) Photoplethysmography-based heart rate monitoring using asymmetric least squares spectrum subtraction and bayesian decision theory. *IEEE Sens J* 15(12):7161–7168
39. Farhadi M, Mashhadi MB, et al (2016) Realtime heart rate monitoring using photoplethysmographic (PPG) signals during intensive physical exercises. *bioRxiv* 092627
40. Sun B, Feng H, Zhang Z (2016) A new approach for heart rate monitoring using photoplethysmography signals contaminated by motion artifacts. In: 2016 IEEE international conference on acoustics, speech and signal processing (ICASSP). IEEE, New Jersey, pp 809–813
41. Zhang Z (2015) Photoplethysmography-based heart rate monitoring in physical activities via joint sparse spectrum reconstruction. *IEEE Trans Biomed Eng* 62(8):1902–1910
42. Zhang Z, Pi Z, Liu B (2014) TROIKA: a general framework for heart rate monitoring using wrist-type photoplethysmographic (PPG) signals during intensive physical exercise. *IEEE Trans Biomed Eng* 9294(c):1–10. URL <http://www.ncbi.nlm.nih.gov/pubmed/25252274>
43. Xiong J, Cai L et al (2016) Spectral matrix decomposition-based motion artifacts removal in multi-channel PPG sensor signals. *IEEE Access* 4:3076–3086
44. Zhao D, Sun Y et al (2017) SFST: a robust framework for heart rate monitoring from photoplethysmography signals during physical activities. *Biomed Signal Process Control* 33:316–324
45. Schäck T, Sledz C et al (2015) A new method for heart rate monitoring during physical exercise using photoplethysmographic signals. In: 23rd European signal processing conference (EUSIPCO), 2015. IEEE, New Jersey, pp 2666–2670
46. Murthy NKL, Madhusudana PC et al (2015) Multiple spectral peak tracking for heart rate monitoring from photoplethysmography signal during intensive physical exercise. *IEEE Signal Process Lett* 22(12):2391–2395
47. Ahamed ST, Islam MT (2016) An efficient method for heart rate monitoring using wrist-type photoplethysmographic signals during intensive physical exercise. In: 5th International conference on informatics, electronics and vision (ICIEV), 2016. IEEE, New Jersey, pp 863–868
48. Temko A (2015) Estimation of heart rate from photoplethysmography during physical exercise using Wiener filtering and the phase vocoder. In: 37th Annual international conference of the IEEE engineering in medicine and biology society (EMBC), 2015. IEEE, New Jersey, pp 1500–1503
49. Salehizadeh S, Dao D et al (2015) A novel time-varying spectral filtering algorithm for reconstruction of motion artifact corrupted heart rate signals during intense physical activities using a wearable photoplethysmogram sensor. *Sensors* 16(1):10
50. Torres JMM, Ghosh A et al (2016) Heal-T: an efficient PPG-based heart-rate and IBI estimation method during physical exercise. In: 24th European signal processing conference (EUSIPCO), 2016. IEEE, New Jersey, pp 1438–1442
51. Chowdhury S, Hyder R et al (2016) Real time robust heart rate estimation from wrist-type PPG signals using multiple reference adaptive noise cancellation. *IEEE J Biomed Health Inform*
52. Fallet S, Vesin J-M (2015) Adaptive frequency tracking for robust heart rate estimation using wrist-type photoplethysmographic signals during physical exercise. In: 2015

- Computing in cardiology conference (CinC), IEEE, New Jersey, pp 925–928
53. Khan E, Al Hossain F et al (2016) A robust heart rate monitoring scheme using photoplethysmographic signals corrupted by intense motion artifacts. *IEEE Trans Biomed Eng* 63(3):550–562
  54. Mashhadi MB, Asadi E et al (2016) Heart rate tracking using wrist-type photoplethysmographic (PPG) signals during physical exercise with simultaneous accelerometry. *IEEE Signal Process Lett* 23(2):227–231
  55. Fallet S, Vesin J-M (2017) Robust heart rate estimation using wrist-type photoplethysmographic signals during physical exercise: an approach based on adaptive filtering. *Physiol Meas* 38(2):155
  56. Alqaraawi A, Alwosheel A, Alasaad A (2016) Towards efficient heart rate variability estimation in artifact-induced Photoplethysmography signals. In: *IEEE Canadian conference on electrical and computer engineering (CCECE)*, 2016. IEEE, New Jersey, pp 1–6
  57. Alqaraawi A, Alwosheel A, Alasaad A (2016) Heart rate variability estimation in photoplethysmography signals using Bayesian learning approach. *Healthc Technol Lett* 3:136–142
  58. Kazmi SA, Khan S et al (2015) Spectrum analysis of physiological signals of human activities. In: *International conference on emerging technologies (ICET)*, 2015. IEEE, New Jersey, pp 1–6
  59. Wang Y, Liu Z, Dong B (2016) Heart rate monitoring from wrist-type PPG based on singular spectrum analysis with motion decision. In: *IEEE 38th annual international conference of the engineering in medicine and biology society (EMBC)*, 2016. IEEE, New Jersey, pp 3511–3514
  60. Mullan P, Kanzler CM et al (2015) Unobtrusive heart rate estimation during physical exercise using photoplethysmographic and acceleration data. In: *37th Annual international conference of the IEEE engineering in medicine and biology society (EMBC)*, 2015. IEEE, New Jersey, pp 6114–6117
  61. Hayashi T, Ooi T (2016) Estimation of heart rate during exercise from a photoplethysmographic signal considering exercise intensity. *Sens Mater* 28(4):341–348
  62. Zheng Y, Poon CC et al (2016) Pulse arrival time based cuff-less and 24-h wearable blood pressure monitoring and its diagnostic value in hypertension. *J Med Syst* 40(9):195
  63. Allen J (2007) Photoplethysmography and its application in clinical physiological measurement. *Physiol Meas* 28(3):R1
  64. Jarchi D, Casson AJ (2016) Description of a database containing wrist PPG signals recorded during physical exercise with both accelerometer and gyroscope measures of motion. *Data* 2(1):1
  65. Pu L, Chacon PJ et al (2017) Novel tailoring algorithm for abrupt motion artifact removal in photoplethysmogram signals. *Biomed Eng Lett* 1–6
  66. Standard A (1993) Z136. 1. American national standard for the safe use of lasers. American National Standards Institute. Inc, New York



**Vijitha Periyasamy** is a research staff in the School of Chemical and Biomedical Engineering, Nanyang Technological University, Singapore. She has a bachelor's degree in medical electronics from Visvesvaraya Technological University, India. Her

research interests include biomedical image processing for clinical evaluation, development of multimodal imaging systems, Monte Carlo simulation for light transport in biological tissue, and application of bioengineering for different medical practice systems.



**Manojit Pramanik** received his Ph.D. degree (2010) in Biomedical Engineering from Washington University in St. Louis, St. Louis, USA. He joined the School of Chemical and Biomedical Engineering (SCBE) at Nanyang Technological University (NTU), Singapore as an Assistant Professor in January 2014. He obtained his masters (M.Tech.) degree from Department of Instrumentation at Indian Institute of Science (IISc), Bangalore, India in 2004. He did his undergraduate (B.Tech) from the Department of Electrical Engineering at Indian Institute of Technology (IIT), Kharagpur, India in 2002. His research interests include development of

photoacoustic and thermoacoustic imaging systems, image reconstruction methods, clinical application areas such as breast cancer imaging, molecular imaging, contrast agent development, Monte Carlo simulation for light transport in biological tissue etc. He has more than 120 international journal and conference publications and presentations.



**Prasanta Kumar Ghosh** received his Ph.D. in Electrical Engineering from University of Southern California (USC), Los Angeles, USA in 2011. Prior to that, he obtained his M.Sc.(Engineering) in Electrical Communication Engineering from

Indian Institute of Science (IISc), Bangalore and B.E.(ETCE) in Electronics from Jadavpur University, Kolkata in 2006 and 2003, respectively. He has been a Research Intern at Microsoft Research India, Bangalore in the area of audio-visual speaker verification from March to July in 2006. During 2011–2012, he was with IBM India Research Lab (IRL) as a researcher. Currently, he is an Assistant Professor in the department of Electrical Engineering (EE) at IISc. Before joining as assistant professor, he was a faculty fellow in the department of EE under the INSPIRE faculty fellowship program.